Solvent, Temperature, and Excitonic Effects in the Optical Spectra of Pseudoisocyanine Monomer and J-Aggregates

Indrek Renge* and Urs P. Wild

Physical Chemistry Laboratory, ETH-Zentrum, CH-8092 Zürich, Switzerland

Received: April 22, 1997; In Final Form: June 18, 1997[⊗]

The absorption and fluorescence spectra of 1,1′-diethyl-2,2′-cyanine (pseudoisocyanine, PIC) aggregates have been studied between 8 and 293 K in water/glycerol glass containing 2−4 M of alkali halogenides. In this system the J-aggregates have a single sharp band and there is practically no contamination with the monomeric dye, dimers, or H-aggregates. This allowed us to better resolve the high-energy portion of the spectrum and to assign the middle 535 nm band to the upper exciton transition. The excitonic splitting at 8 K is the same for both the blue and the red forms of aggregates (1270 ± 10 cm^{-1}). The average energy of exciton components (18195 ± 15 cm^{-1} for the blue form) was found to be very close to the 0−0 energy of the first strong site of PIC monomer (18223 cm^{-1}) embedded in a 9-aza-PIC iodide matrix, which is transparent above 500 nm [Marchetti, A. P.; Scozzafava, M. *Chem. Phys. Lett.* **1976**, *41*, 87]. The 0−0 frequency of the nonsolvated PIC monomer cation (ν_0^0 = 19716 ± 40 cm^{-1} or 507.2 ± 1 nm) was obtained from the solvent shift measurements at room temperature. The absorption bandwidths and shifts of both the PIC cation in poly(methyl methacrylate) matrix and the aggregates were recorded in the temperature range between 8 and 300 K. The thermal shift of band maxima was analysed in terms of the change in dispersive shift and excitonic splitting as a result of the expansion of the matrix and a pure thermal or phonon-induced contribution. The thermal shift and broadening behavior of molecular and excitonic transitions reveals large differences in the mechanism and strength of the coupling to low-frequency vibrations.

Introduction

The optical spectra of 1,1′-diethyl-2,2′-cyanine (pseudoisocyanine, PIC) in red-shifted aggregated forms are remarkably intense and narrow for an organic system at ambient temperature. After the discovery of this phenomenon in 1937,[1,2] the spectroscopic properties of PIC aggregates (also referred to as J-aggregates) were exhaustively studied by Scheibe and coworkers.[3−10] Interestingly, Jelly made his observations in organic media,[1] whereas Scheibe used mostly aqueous solutions of PIC. It was noticed in the very first papers that the sharp transitions are atomic-like with their absorption and fluorescence nearly in resonance,[1,2] and therefore, very weakly coupled to molecular vibrations.[6] It was emphasized that the electronic excitation should be delocalized over many molecules, since mixed aggregates of two different dyes give a single band.[3] The energy splitting effect in a system of coupled oscillators and the selection rules for optical transitions as a function of the mutual orientation of the oscillators were proposed already in 1948 (before the works of Davydov and Kasha, see refs 11 and 12 and references therein), and the blue or red shifts of absorption bands in dimers and higher aggregates were explained.[8] Many cyanine dyes similar to PIC were synthesized and the influence of structure on the capability to "polymerize" was investigated.[4,7] Later, in several theoretical papers the spectral shift, narrowing, and the vibronic structure of the aggregates were treated quantitatively.[13−16]

The shift and narrowing of J-bands upon cooling with liquid air was reported as early as in 1944.[17] However, most of the low-temperature and laser spectroscopy has been carried out within the last 10 years. Optical dephasing in J-transitions was characterized by means of photon echo methods.[18−20] Spectral hole-burning measurements have confirmed that the J-bands consist largely of purely electronic zero-phonon transitions with inhomogeneously distributed frequencies.[18,21−24]

Most of the advanced spectroscopic investigations at low temperatures[18−24] have been performed in the vitreous water/ethylene glycol mixture proposed by Cooper in 1970.[25] In this matrix the study of higher exciton components is difficult, because of the overlap with the absorption of monomers, dimers, and H-aggregates. The analysis of absorption spectra is further complicated by the fact that two narrow features appear upon cooling. This doublet structure has been ascribed to different stacking configurations of PIC molecules in the aggregate.[26]

It will be shown in this paper that essentially complete aggregation of PIC at temperatures below 300 K can be achieved in a glass-forming mixture of 50% (by weight) glycerol with water in the presence of high concentrations (1−4 M) of alkali halide salts. A single *J*-peak emerges accompanied by two broad satellite bands at ∼535 and ∼495 nm. We present much evidence that the second, 535 nm band can belong to the upper exciton transition.

In the first subsection of Results and Discussion section, the absorption spectra of PIC monomers in a number of liquids and polymers at 293 K will be discussed. The solvent shift mechanism, the transition energy of the free PIC cation and the polarizability change at $S_1 \leftarrow S_0$ excitation will be established according to refs 27 and 28. In the next section the assignment of upper exciton band is done. The magnitude of excitonic splitting and the vacuum-to-aggregate frequency shift in the low-temperature limit are estimated. Furthermore, the vibronic structure of both exciton bands is analyzed in terms of current theoretical models.[15,16] The lower exciton transition is characterized not only by a dramatic band narrowing but also by a

[⊗] Abstract published in *Advance ACS Abstracts,* September 15, 1997.

S1089-5639(97)01371-6 CCC: $14.00

considerable reduction of vibronic activity (subsection 3). The inhomogeneous bandwidths of the PIC monomer and the aggregates are discussed in subsection 4. The difficulties in separating the influence of motional narrowing and the structural order will be pointed out. In the following, the manifestations of quadratic vibronic interactions, the thermal band broadening (subsection 5), and shift are dealt with in terms of electron−phonon coupling (EPC). The PIC molecular band shift in a polymer host is separated into the solvent shift and pure thermal shift components by using the thermal expansion coefficient of the matrix (subsection 6).[29] Furthermore, the observed temperature-induced shift of both exciton components is split into dispersive, phonon-induced and resonant parts by making use the X-ray data on thermal expansion of a crystalline polymethine dye (subsection 7).[30] Finally, the ratio of thermal shift to the broadening of spectral bands for PIC cation and aggregate is compared to that for the other π-electronic transitions in doped polymers and are found to be very sensitive with respect to the strength of electron-phonon coupling. The general interdependence of solvent shift phenomena, vibronic coupling and excitonic interaction will be explored. A preliminary account of this work has been published in the proceedings of the 2nd Exciton Conference.[31]

Experimental Section

Polymers (except for poly(methyl methacrylate), PMMA) and 1,1′-diethyl-2,2′-cyanine iodide were purchased from Aldrich. PMMA was a commercial Plexiglass. To prepare a doped film, the polymer and PIC were dissolved in CH_2Cl_2, and the solution was cast in a Petri dish and let to dry. Solvent was removed by heating at 60 °C under vacuum for 20 h. Aggregates were prepared by mixing an aliquot of the 2×10^{-3} M stock solution of PIC iodide in 86−88% glycerol (Fluka, puriss) with an equal volume of highly concentrated aqueous solution (4−6 M) of salts (KF, KCl, KBr, and NaCl). Concentrations indicated in the text refer to the samples at room temperature. The solutions were placed between two quartz plates (~3 μm layer) for fluorescence measurements or in 10 or 100 μm Hellma cells for absorption scans, and the solutions were frozen rapidly in liquid N_2. At room temperature the gelation takes place during several minutes, but it can be reverted by warming up the solution. In thin layers the solution remains transparent during tens of minutes or longer. The quickly frozen samples were transferred to Oxford CF204 or CF1204 continous flow cryostats. Absorption spectra were recorded on Perkin-Elmer Lambda 9 spectrophotometer. Calibration was made with the aid of 0.25 M solution of $HoCl_3$ in 0.1 M HCl having sharp bands at 416.1, 536.5, and 640.5 nm. Aggregate spectra were measured with different slit widths between 0.1 and 2 nm, and the corrected bandwidth was obtained by extrapolation to zero slit width. Fluorescence spectra were measured on a computer-controlled total luminescence spectrometer, assembled on the basis of two Spex1402 double-grating monochromators (dispersion 0.5 nm/1 mm slit width), an Osram XBO 2.5 kW high-pressure Xe lamp, a Peltier-cooled Hamamatsu R2949 photomultiplier, and a Stanford SR400 two-channel gated photon counter. Monochromators were calibrated with Kr and Hg Pen-Ray lamps from Oriel Spectral Calibration Set, model C-13-02. Emission spectra were not corrected with respect to the sensitivity of the setup. However, the response curve of the R2949 photomultiplier is rather flat with its quantum efficiency decreasing by a factor of 1.6/100 nm between 300 and 800 nm. Temperature was established with Oxford ITC4 controller and monitored close to the sample with Lake Shore Cryotronics 201 silicon diode thermometer.

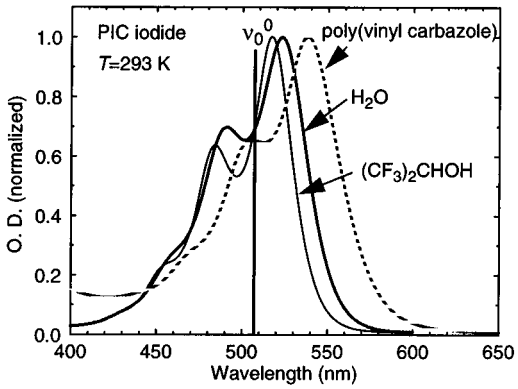

Figure 1. Absorption spectra of monomeric 1,1′-diethyl-2,2′-cyanine iodide at room temperature. The vertical bar shows the position of the electronic origin for nonsolvated dye cation in vacuum obtained by extrapolation of eq 1.

Results and Discussion

1. Matrix Dependence of Absorption Band Maxima of Monomeric PIC at 293 K. The visible absorption of the PIC cation shows a strong 0−0 band accompanied by two resolved vibronic satellite bands (Figure 1). The 0−0 band maxima (ν_m) and half-widths at half-maxima (hwhm) for the red side of the band were determined in liquid solvents and polymers of various polarities and polarizabilities (Table 1). A linear relationship holds between ν_m and the matrix polarizability function $\phi(n^2) = (n^2 - 1)/(n^2 + 2)$, n is the refractive index for the Na D line (Figure 2):

$$\nu_m = (19716 \pm 40) - (2964 \pm 147)\phi(n^2), \quad N = 31, \quad r = 0.966 \quad (1)$$

where N is the number of data points and r is the correlation coefficient. Hexafluoro-2-propanol, trifluoroethanol, dioxane, and iodomethane were excluded from the regression.

Good overall linearity of eq 1 means that the largely predominating mechanism of the solvent shift is the dispersive stabilization of the excited state relative to the ground state in both liquid and solid environment.[37] In fluorinated alcohols the solvent shift is less than expected on the basis of n. The polarizability density of fluorine atoms is less than that of hydrogen and carbon. Thus the impurity molecule appears to be screened from the more polarizable carbon backbone by relatively large F atoms and the effective interaction radius (Onsager cavity radius) increases as a result of such an anisotropy.[27] On the average, the solvent shift in polymers is also less by ~30 cm^{-1}. Perhaps the space filling around the dye molecule is less tight in a macromolecular host and, as a result, the solvent shift slightly decreases. A bathochromic deviation from eq 1 in dioxane and iodomethane may be due to ion association effects, since these media have low dielectric constants (ϵ) (Table 1). The influence of hydrogen bonding properties and polarity, as well as that of quadrupolar moments of aromatic solvent molecules (pyridine, benzonitrile, and nitrobenzene), on absorption maxima of PIC is nearly negligible.

Absorption band shifts of PIC and other monomethine and carbocyanine dyes in a large variety of liquids have been studied and plotted vs the function $f(n^2) = (n^2 - 1)/(2n^2 + 1)$.[38] It has been established that both functions $\phi(n^2)$ and $f(n^2)$ yield good linear fits.[38] The slope (p) value recalculated from these data is slightly larger ($-p = 3420$ cm^{-1}) than that of eq 1, because of the inclusion of several less polar solvents in ref 38.

The pressure shifts amounting from −35 to −125 cm^{-1} (between 0 and 10 kbar) have been published for many

TABLE 1: Absorption Band Maxima and Widths of Pseudoisocyanine Iodide at 293 K[a]

no.	solvent	n	$\phi(n^2)$	ϵ	$19\,716 - \nu_m$ (cm^{-1})[b]	$\Delta\nu$ (cm^{-1})[c]	2hwhm (cm^{-1})[d]
			very polar ($\epsilon > 30$) aprotic solvents				
1	acetonitrile	1.3441	0.2119	37	629	−1	1198
2	nitromethane	1.3817	0.233	38	692	−1	
3	propylene carbonate	1.4189	0.252	66	733	14	
4	*N*,*N*-dimethylformamide	1.431	0.2588	38.7	803	−36	
5	γ-butyrolactone	1.4365	0.262	39	776	1	
6	dimethyl sulfoxide	1.479	0.2836	47.2	873	−32	
7	sulfolan	1.4840	0.286	44.5	822	26	1190
8	furfural	1.5262	0.307	42.1	916	−6	
9	nitrobenzene	1.5562	0.322	35.7	985	−31	
			less polar ($\epsilon < 30$) aprotic solvents				
10	acetone	1.3588	0.220	21.4	667	−15	
11	dichloromethane	1.424	0.2552	8.9	790	−34	
12	dioxane	1.4224	0.2582	2.22	888	−123	1252
13	1-bromopropane	1.4336	0.2602	7.66	841	−70	
14	cyclopentanone	1.437	0.2620	13.6	793	−16	
15	epichlorhydrin	1.438	0.2625	22.6	800	−22	
16	1,2-dichloroethane	1.445	0.2662	10.5	821	−32	
17	chloroform	1.446	0.2667	4.81	805	−15	
18	pyridine	1.510	0.2991	13.55	907	−20	
19	benzonitrile	1.528	0.3079	25.6	932	−19	
20	iodomethane	1.531	0.3094	7.0	1035	−118	1234
			hydrogen-bonding solvents				
21	hexafluoro-2-propanol	1.2750	0.1726	16.7	377	135	1025
22	trifluoroethanol	~1.30	~0.187	27.7	411	143	1060
23	methanol	1.329	0.2034	33.52	609	−6	
24	water	1.3330[e]	0.2057	81.2	596	14	1208
25	ethanol	1.360	0.2207	25.3	650	4	
26	50% (w/w)glycerol/water	1.3983[e]	0.245		688	38	1158 764[f]
27	*N*-methylformamide	1.432	0.2594	189	776	−7	
28	1-dodecanol	1.440[g]	0.2636	6.8[h]	781	0	1224
29	formamide	1.447	0.2672	111.8	759	33	
30	90% glycerol	1.4583[e]	0.271		758	51	1108
			polymers				
31	poly(vinyl acetate)	1.4665[i]	0.277		746	75	1190
	cellulose triacetate	1.475[i]	0.282		841[j]	−5	
32	poly(vinyl butyral)	1.485[i]	0.2866		812	37	1202
33	poly(methyl methacrylate)	1.490[i]	0.289		828	29	1330 1071[f]
34	polycarbonate	1.5850[i]	0.335		963	30	1562
35	poly(vinyl carbazole)	1.683[i]	0.379		1131	−8	1410

[a] n, refractive index for Na D line at 293 K from ref 32; $\phi(n^2) = (n^2 - 1)/(n^2 + 2)$; ϵ, dielectric constant at 293 K from ref 33. [b] Absolute solvent shift: band maximum relative to the extrapolated transition frequency of a nonsolvated dye, error ±3 cm^{-1}. [c] Deviation from the regression line, eq 1. [d] Double value of the half-width at half-maximum for the long-wavelength side of the band, error ±5 cm^{-1}. [e] Reference 34. [f] At 10 K. [g] For 2-dodecanol. [h] At 25 °C. [i] Reference 35. [j] Reference 36.

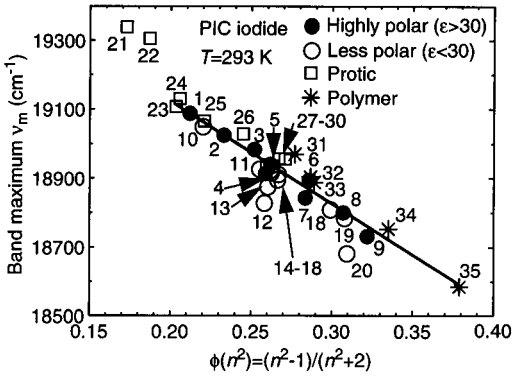

Figure 2. Dependence of the 1,1′-diethyl-2,2′-cyanine iodide absorption maximum at room temperature on the polarizability function of the matrix, $\phi(n^2) = (n^2 - 1)/(n^2 + 1)$. The numbers of solvents and polymers correspond to those in Table 1.

symmetric and asymmetric cyanines including PIC (−70 cm^{-1}) up to very high pressures of 140 kbar.[36] For the sake of comparison with solvent shifts, it is useful to present the pressure-shift data as a function of $\phi(n^2)$. According to the Lorentz−Lorenz formula, $\phi(n^2)$ is linearly related to density d:[39]

$$\phi(n^2) = (4\pi N_A \alpha/3M_w)d \qquad (2)$$

where N_A is the Avogadro constant, M_w is the relative molecular weight, and α is the molecular polarizability. From the refractive index of cellulose triacetate $n = 1.47 - 1.48$[35] at ambient conditions and the volume compression at 10 kbar $\Delta V/V_0 = 0.1189$,[40] the change of $\phi(n^2)$ between 0 and 10 kbar can be obtained:

$$\Delta\phi(n^2) = \phi(n^2)(\Delta V/V_0)/[1 - (\Delta V/V_0)] = 0.038 \qquad (3)$$

The pressure shift per unit Lorentz−Lorenz function $-p' = 70/0.038 = 1840$ cm^{-1} turns out to be somewhat smaller than $-p = 2964$ cm^{-1} (eq 1).

The change of static polarizability between the ground and the excited state $\Delta\alpha$ can be estimated from the Bakhshiev formula[37] or an empirical expression:[28]

$$\Delta\alpha = -(0.4 \pm 1.5) - (18.4 \pm 4) \times 10^{-6}\, pM_w \qquad (4)$$

where the relative molecular weight M_w is used as a cavity size parameter. With $p = -2964$ cm^{-1} and M_w of the PIC cation

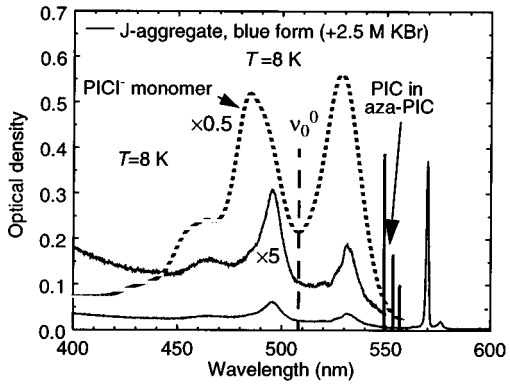

Figure 3. Low-temperature absorption spectra of PIC iodide monomer (2×10^{-4} M, 0.5 mm cell) (dotted line) and the blue form of J-aggregates (10^{-3} M PIC in the presence of 2.5 M KBr, 10 μm cell) (thin lines) in 50% glycerol/water glass. As evidenced from the larger intensity of the 485 nm band (see Figure 1) some PIC dimer is formed upon freezing the diluted solution. Bands belonging to upper excitonic transition are shown also in an enlarged scale (5×). Vertical bars indicate the positions of zero-phonon lines of PIC impurity in aza-PIC crystal at 548.77, 552.6, and 555.75 nm from ref 41. Position of the 0−0 origin of PIC monomer in vacuum is shown with a dotted bar.

being 327.5, one obtains $\Delta\alpha = 17 \pm 3$ Å^3. This value is only slightly smaller than $\Delta\alpha$ for cyclic polymethine cations (rhodamines and oxazines) (18−27 Å^3) or ^1L_a (p) transitions in polycyclic arenes with comparable molecular size (18−22 Å^3).[28]

Extrapolation of solvent polarizability $\phi(n^2)$ in eq 1 to zero yields the frequency values (ν_0) which are close to purely electronic origins (ν_0^0) in cold molecular beams.[27] Even for the spectra composed mainly of progressions of low-frequency modes, such as the ones of tetraphenylporphine, tetraphenyltetracene (rubrene), and coumarin 152A(481), the intercept ν_0 was found to be very close to the 0−0 origin in these flexible chromophores.[27] Therefore, the 0−0 transition energy of PIC cation in a nonsolvated state is expected to lie close to 19 716 cm^{-1} (507.2 nm). In contrast to some other dyes,[27] no correction for polarity is needed because the PIC spectrum is insensitive towards the dielectric constant.[61] Measuring the ν_0^0 values for bare dyes in their ionic form in supersonic molecular beams would be associated with serious difficulties as a result of ion pair formation in the gas phase.

PIC iodide embedded in a single crystal of 1,1′-diethyl-9-aza-2,2′-cyanine iodide (aza-PIC) shows the strongest zero-phonon line at 18 223 cm^{-1} (548.77 ± 0.05 nm) at 1.8 K.[41] According to eq 1 the solvent shift of this peak is −1493 cm^{-1}, which corresponds to the Lorentz−Lorenz function value of 0.504 and the effective refractive index $n = 2.012$. To our knowledge, no n or ϵ values for the host crystal have been published. The n value about 2 seems to be reasonable, as the average n for anthracene is 1.77 (at 546 nm Hg line).[42] The zero-phonon frequency of PIC in aza-PIC crystal host may be taken as a hypothetical value for monomers in J-aggregate in the absence of excitonic interaction.

2. Band Assignment in the Spectrum of J-Aggregates. Absorption spectra of 1×10^{-3} M PIC iodide in 50% aqueous glycerol at 8 K are shown in Figures 3−5. The sharp J-bands appear at 570.03 nm (blue form) and 576.4 nm (red form) in the presence of 2.5 M KBr or 4 M KF, respectively. Upon addition of 2 M NaCl or KCl, the blue form of the aggregate with the maximum at 568.9 nm appears (Table 2). Besides the predominating blue line, the solution containing KBr displays also a tiny peak of the red form at 576.9 nm (Figure 3). Therefore, depending on the added anion, both the blue and red forms of aggregates can be prepared selectively. With the increase of polarizability of the anion a small red shift of the

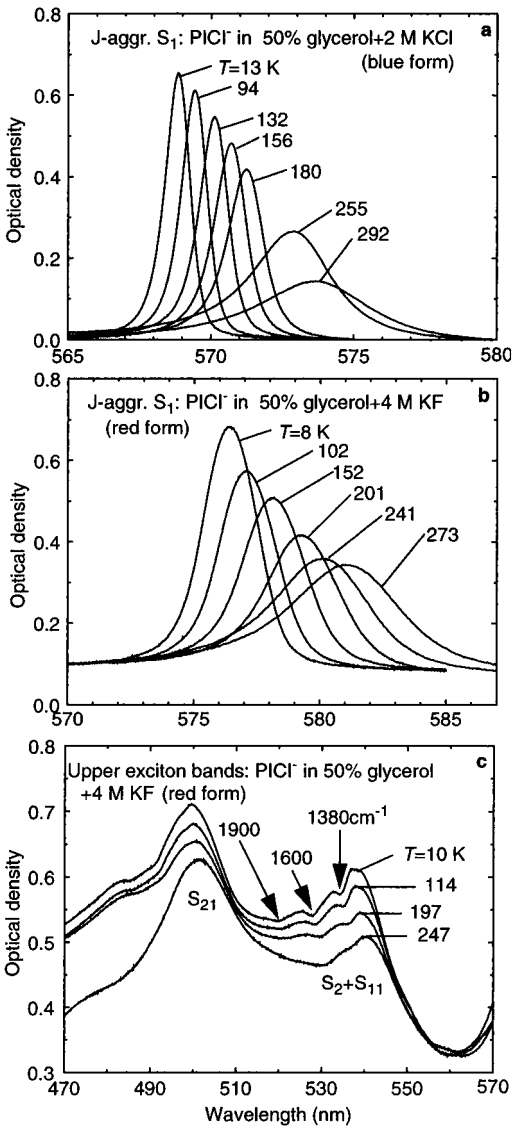

Figure 4. Temperature dependence of the PIC aggregate absorption in 50% glycerol/water glass: (a) J-band of the blue form in the presence of 2 M KCl in a 10 μm cell, absorption level outside the band was set to zero; (b) J-band of the red form in the presence of 4 M KF in a 10 μm cell, (c) the same for the upper exciton bands in a 100 μm cell. The position of holes in the S_2 band relative to the J-band maximum are shown in cm^{-1} units by arrows (part c). Temperatures of the measurement are indicated at each curve.

J-peak takes place: 1 nm between Cl^- and Br^- in the blue form and 0.5 nm between F^- and Br^- in the red form.

The J-bands are accompanied by two broad features with maxima approximately at 495 and 535 nm. These maxima are close to the positions of the S_1 band and its first vibronic satellite of predominately monomeric PIC in the same solution without added salt (Figure 3), but the widths and relative intensities of these bands in the monomer and aggregate spectra are very different. The absorption and fluorescence excitation spectra of J-aggregates between 450 and 550 nm are very similar (Figure 5). Therefore, the 495 and 535 nm bands belong to aggregates. In contrast to vitrified salt-free aqueous ethylene glycol,[18−26] the glycerol/water/halogenide system yields spectroscopically pure single-type J-aggregates devoid of contamination with monomeric, dimeric, or H-aggregated species. However, a spectrum of fully aggregated PIC in 1:1 mixture of water and ethylene glycol develops at room temperature under the pressure of 7 kbar.[43] It is of interest that a concentrated solution ((1−3) $\times 10^{-2}$ M) of PIC in water has also a spectrum of pure

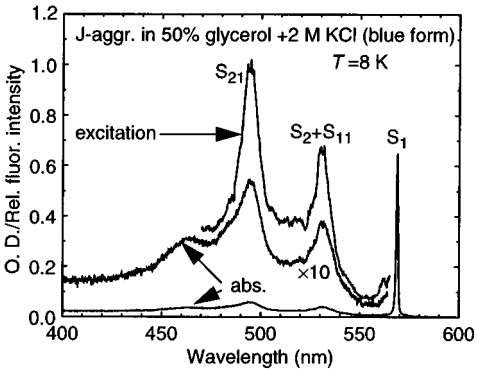

Figure 5. Absorption and fluorescence excitation spectra of PIC (10^{-3} M) J-aggregates in 50% glycerol in the presence of 2 M KCl (blue form), $T = 8$ K. The solution was placed in a 10 μm silica cell or between silica plates (3 μm layer) for absorption and excitation measurements, respectively. The optical density at 600 nm was set to 0. The high-energy portion of the absorption spectrum is shown in an enlarged scale (×10). Excitation spectrum was recorded close to the emission maximum (569.4 nm) with 0.3 nm slits.

aggregate.[3,9,10] Clean aggregate spectrum appears also in thin films of low-molecular weight poly(vinyl alcohol) containing about 10% (2−3 M) of PIC.[44,45]

The prominent satellite bands are displaced from the J-band maxima by 1270 ± 10 cm^{-1} and 2640 ± 20 cm^{-1} (2720 ± 30 cm^{-1} in the red form). There is no shift in the 535 nm band region in the excitation spectra when the narrow-band recording (slit width 0.2 nm) is tuned over the inhomogeneously broadened J-band (data not shown). On the other hand, there is lack of mirror symmetry with respect to the intensities of the 535 nm band and the vibronic fluorescence of the J-band having the relative intensity as small as 18 ± 5% of the resonance intensity (Figures 3, 5, and 6). By contrast, the integrated absorption area of the 530 nm band (500−1700 cm^{-1} above the 0−0) relative to the J-band is 45 ± 5% for the red form or even as large as 100 ± 15% for the blue form. In dichroic absorption spectra of oriented aggregates the short-wavelength bands exhibit a different polarization than the J-band.[5,9,44,45] The 572 nm band, on one hand, and the 530 and 494 nm bands, on the other hand, have different signs in the circular dichroism spectra in an aqueous solution of 1.5 × 10^{-3} M PIC and 1 M dipotassium L(+)-tartrate at room temperature.[10]

All these observations can be understood by assuming that the short-wavelength bands belong to a different electronic transition, rather than to vibronic subbands of the lower transition. The zero-phonon lines (ZPLs) of PIC embedded in the transparent aza-PIC crystal at 548.77, 552.6, and 555.75 nm[41] lie just between the narrow band and its first satellite (Figure 3). Therefore, there is good reason to assume that the 535 nm feature belongs mainly to the transition to the top of the excitonic band or to the upper level of a symmetrically split exciton component. We propose that the 535 nm band consists mainly of the upper exciton component (from here on denoted as S_2) and the stronger peak at 495 nm incorporates its vibronic sub-band (S_{21}). It was deemed earlier that the S_{21} band may be due to the upper exciton transition.[15] The less intense S_2 has been occasionally ascribed to a vibronic side band of S_1.[15,44,45]

Figure 7 illustrates how the energy levels of PIC aggregates develop starting from the cold PIC monomer in vacuum. An average 1500 cm^{-1} shift occurs between the 0−0 origin in bare PIC monomer and the zero-phonon lines in diluted aza-PIC host matrix as a result of the change in the interaction energy of one molecule with all the rest in its transition to an excited state. This matrix shift has been taken into account phenomenologically in the theory of molecular excitons.[11,12] The energy down shift results largely from the dispersive stabilization of the S_1 state relative to the ground state owing to the higher polarizability of the former. In neat PIC the solvent shift must be close to that in aza-PIC, since the resonance interaction leads to a nearly symmetric level splitting by 1270 ± 10 cm^{-1} relative to the monomer peak at 18223 cm^{-1} in the aza-PIC crystal.[41] Similarly, the A_u-B_u Davydov splitting of 1700 ± 400 cm^{-1} has been derived for the (201) face from the absorption contours of PIC iodide crystal, obtained by Kramers−Kronig transformation of reflection spectra at 173 K.[46] With the increase of temperature up to 293 K both exciton levels are shifted by ∼150 cm^{-1} to lower energies (see below).

3. Vibronic Structure in the Spectra of PIC Monomer and Aggregate. In this subsection the vibronic structure and intensities in absorption and fluorescence spectra will be treated in more detail for both PIC monomers and J-aggeragates. In contrast to those of the J-aggregate, the vibronic intensities in the fluorescence and excitation spectra of the diluted monomer solution are similar (Figure 8). The two vibronic satellite bands are less resolved in fluorescence because of the broadening, but the two harmonics of the ∼1400 cm^{-1} modes are clearly discernible. Our attempts to resolve the vibronic structure by tuning the narrow-band (0.5 nm) excitation to the red edge of the PIC 0−0 absorption band failed. However, the site-selection effect can be demonstrated in PIC aggregates. The excitation in resonance with the J-band produces an emission spectrum displaying numerous lines between 200 and 1600 cm^{-1} (Figure 9).

In the absorption and excitation spectra of aggregates, a spectacular structure is observed in the S_2 band region in the frequency interval 1300−2000 cm^{-1} above the J-band, consisting of several shallow holes on a broad background (Figures 4c and 9). The minima of the holes are displaced from S_1 by 1380, 1550−1600, and 1800−1900 cm^{-1} and resemble the 1370 and 1630 cm^{-1} peak positions in the emission spectra (Figure 9). Similar structure can be discerned in published low-temperature absorption spectra of PIC aggregates,[24,25] but as far as we know, its origin has been never discussed. One can speculate that peculiar resonance effects may occur when the S_1 vibrational levels fall in the S_2 purely electronic exciton zone. An alternative explanation might be that groups of S_1 vibrational lines centered at 1270, 1470, 1650, and ∼2000 cm^{-1} can make up broad features and leave narrower gaps between them. However, this possibility can be discarded because of the fact that any shifts in the S_2 region are absent in the excitation spectra recorded with narrow bandpass detection (slit width 0.2 nm) within the inhomogeneously broadened fluorescence band between 568.5 and 569.5 nm (blue form, 2 M KCl). In particular, the hole at 522.8 ± 0.2 nm (Figure 5) is not shifting with the displacement of the detection wavelength (data not shown). Thus, the absorption intensity modulation within the S_2 band is characteristic to the upper excitonic transition itself.

The strong and broad S_{21} band is separated from S_2 by 1380 ± 20 cm^{-1} and can be tentatively assigned to a group of vibrations of the upper excitonic transition. Accordingly, the temperature shifts of the S_2 and S_{21} bands are similar (Figure 4c and Table 2).

The theory of vibronic coupling in linear PIC aggregates predicts the relative side band intensities of 0.15 and 3 for the excitonic transitions to the lower and upper band edge, respectively (ref 15, p 280). These values are in full accordance with the observed ones (Figures 3, 5, and 6). Moreover, the model of cyclic linear aggregates with two monomers per unit cell provides a correct sequence of transition energies: $S_1 \ll$

TABLE 2: Fitting Parameters of the Temperature Dependence of Band Shifts ($\Delta\nu_m$) in PIC Monomer and J-Aggregates

species	matrix	transition	ν_m (10 K) (cm^{-1})[a]	shift type	$\Delta\nu_m$ (190 K) (cm^{-1})[a]	$\Delta\nu_m$ (293 K) (cm^{-1})[a]	$\Delta\nu_m = a_0 + a_1 T^{a_2}$ a_0 (cm^{-1})	$-a_1$	a_2	ΔT[b] (K)
monomer	PMMA	S_1	18905 ± 3	observed	3	−13	0.6	-7.2×10^{-6}	2.53	9−324
				dispersive[c]	15	32	0	0.0029	1.64	0−324
				pure therm[c]	−19	−44	0.4	-10^{-3}	1.88	0−324
J-aggregate (blue form)	glycerol/H_2O (50%) + 2 M KCl	S_1	17579 ± 0.4	observed	−83	−147	5.8	−0.039	1.46	13−294
							2.0	−0.0017	2.06	13−190
J-aggregate (blue form)	glycerol/H_2O (50%) + 2.5 M KBr	S_1	17543 ± 1	observed	−73		0.9	−0.0031	1.92	8−190
		S_2[d]	18823 ± 3	observed	−55		0.7	−0.0027	1.89	8−190
		S_{21}[e]	20188 ± 3	observed	−45		0.7	−0.0089	1.63	8−190
J-aggregate (red form)	glycerol/H_2O (50%) + 4 M KF	S_1	17350 ± 0.5	observed	−78	−156[f]	2.8	−0.0176	1.60	8−275
							0.7	−0.0041	1.88	8−190
				dispersive[g]	56	96	1.47	0.079	1.25	0−300
				pure therm[g]	−153	−287[f]	−0.1	−0.080	1.44	0−300
				excitonic[g]	20	35	0.5	0.029	1.24	0−300
		S_2[d]	18609 ± 5	observed	−47	−142[f]	−3.8	−0.00019	2.38	8−247
							0.6	−0.019	1.49	8−190
				pure therm[g]	−89	−203[f]	−7.2	−0.0024	1.99	0−300
				excitonic[g]	−20	−35	−0.5	−0.029	1.24	0−300
		S_{21}[e]	20016 ± 5	observed	−42	−97[f]	0.8	−0.0016	1.94	8−247

[a] ν_m, band maximum; $\Delta\nu_m$, band shift relative to 0 K. [b] Temperature interval of the fitting. [c] Dispersive (calculated from eq 6) and pure thermal components (pure therm.) of the observed thermal shift. [d] The 535 nm band, assigned in this work to the 0−0 transition to the upper excitonic level. [e] Vibronic band of the second excitonic transition at 495 nm. [f] Extrapolated value. [g] Dispersive, pure thermal and excitonic components of the observed thermal shift calculated from eqs 8 and 9.

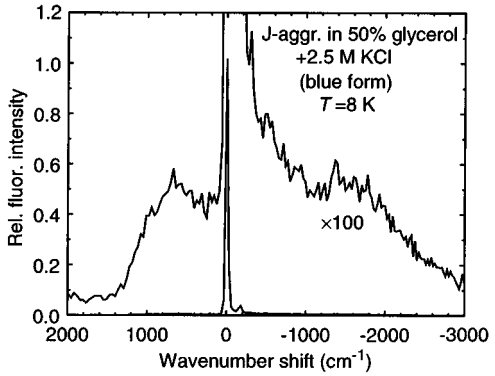

Figure 6. Fluorescence spectrum of PIC (10^{-3} M) J-aggregates in 50% glycerol in the presence of 2.5 M KCl (blue form): excitation wavelength 495 nm with slit width 1.5 nm, recording slit width 0.5 nm, $T = 8$ K. The solution was placed between silica plates (3 μm layer). The spectrum is displayed relative to the J-band maximum (569 nm) in wavenumber scale in order to show that the ~1400 cm^{-1} frequencies predominate in the emisssion as in the case of PIC monomer. The maximum at +600 cm^{-1} (549 nm) belongs to the trace of residual PIC monomer.

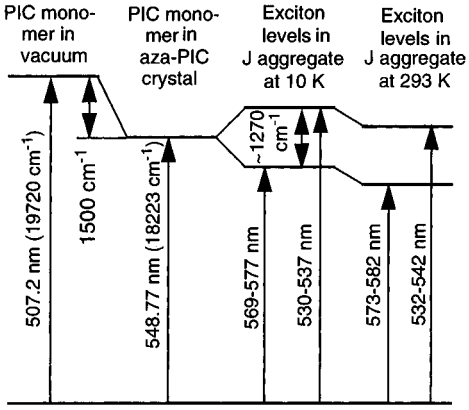

Figure 7. Energy level diagram connecting the 0−0 frequency of the nonsolvated cold PIC molecule (eq 1) with exciton band positions in J-aggregates at room temperature. Arrows indicate the wavelengths for monomeric transitions and band maxima in both blue and red forms of aggregates.

$S_2 < S_{11} \ll S_{21}$.[15,16] In nonoriented samples the upper excitonic band S_2 and the broader vibronic satellite S_{11} of the J-band are not separated. However, the S_2 and S_{11} bands are very well distinguished in absorption dichroism spectra of J-aggregates oriented in a flow of aqueous solution[5,9] or by spin coating of the PIC bromide/poly(vinyl alcohol) in water.[44,45] Both the relative positions and intensities of the calculated spectra (Figures 4 and 6 in ref 15 and Figure 2 in ref 16) for the lower and upper exciton band edge transitions closely resemble the linear dichroism spectra recorded with the light polarization parallel and perpendicular to the flow direction (Figure 1 in ref 15),[9,44,45] respectively. Since the upper exciton band is quite sharp, its position can be correctly measured also in nonoriented samples (Figures 3 and 5).

Let us next discuss the vibronic activity of low-frequency modes hidden within the inhomogenously broadened S_1 band. Fairly large Stokes' shift between the fluorescence and absorption band maxima of monomeric PIC in 50% glycerol/water glass (570 cm^{-1}, Figure 8) reveals strong coupling to low-frequency vibrations. A weak ZPL of PIC monomer in the aza-PIC matrix is accompanied by a huge asymmetric wing spreading between 40 and 340 cm^{-1} (at half-intensity) and peaking at 100 ± 10 cm^{-1} (data taken from Figure 1 in ref 41). These vibrations seem to be characteristic mainly to the chromophore itself rather than to the matrix, because the Stokes' shift in a glass is twice as large as the width of the wing in the crystal (300 cm^{-1}). Both the depth of spectral holes[24] (if we assume saturated holes) and the 0−0 line intensity in the impurity crystal imply that the Debye−Waller factor (DWF) for PIC is about 1%. Here the DWF is defined as an intensity ratio of the ZPL to the total intensity of the whole band under exclusion of high-frequency satellites.

On the contrary to monomeric PIC, the difference between the absorption and fluorescence band contours is barely detectable in J-aggregates (Figure 10). The Stokes' shifts of 4 ± 1 cm^{-1} and 6 ± 2 cm^{-1} were obtained for the blue and red forms, respectively. Accordingly, a pseudo-phonon hole could be burned after a prolonged irradiation of PIC aggregate in glycol/water glass at 568.8 nm that is red-shifted only by 2.5 cm^{-1}.[21] This unusually low-frequency vibration has been attributed to an acoustic mode of the aggregate chain.[21] However, there are at least two alternative explanations of both the Stokes' shift

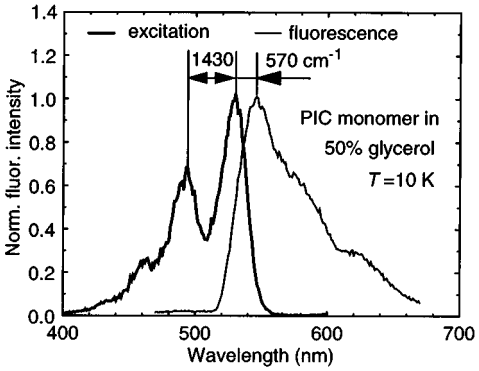

Figure 8. Fluorescence and excitation spectra of 3×10^{-5} M PIC iodide in 50% glycerol, $T = 10$ K. The solution was placed in a 0.5 mm silica cell. The optical density at the 0−0 maximum was 0.1. The emission was excited and the excitation was recorded at the edge of vibronic progession (450 and 670 nm, respectively) in order to suppress the site selection effect. All slits were 1.5 nm. The position of the vibronic satellite band in excitation spectrum (1430 cm^{-1}) and the Stokes' shift between the band maxima (570 cm^{-1}) are indicated. The 2hwhm is 750 and 1100 cm^{-1} for excitation and fluorescence, respectively.

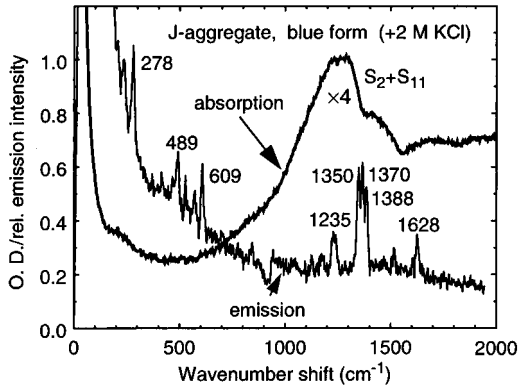

Figure 9. Fluorescence and absorption spectra of J-aggregates in 50% glycerol/water glass (blue form in the presence of 2 M KCl). Fluorescence was excited with narrow slit width (0.3 nm) close to the maximum of the J-band (569.2 nm). Absorption was measured in a 100 μm cell. The spectra are plotted relative to the excitation or J-band maximum frequency to compare the ground-state vibrational frequencies (indicated in cm^{-1}) in the emission spectrum with the structural features of the absorption in the upper exciton region.

and the occurrence of the pseudowing. First, the lowest exciton transition may consist if several closely spaced levels. Second, there may be nearly resonant dipole−dipole energy transfer between different aggregate species within the inhomogeneously broadened ensemble. Both the energy transfer and intraband relaxation may, in principle, account for the observed phenomena. The DWF estimated from the saturated hole depth[21] in the J-bands ought to be at least 0.3. It is probably higher because not all the centers can be subject to photobleaching.

4. Inhomogeneous Bandwidth of PIC Monomer and J-Aggregates. The full width at half-maximum (fwhm) of J-bands at 8 K ranges from 30 to 78 cm^{-1} for the blue and red forms of spectrally pure aggregates (Figure 4a,b, Table 3), respectively. The fwhm of the exciton bands in the blue (571 nm) and the red (578 nm) forms coexisting in ethylene glycol/water glass has been given in the caption of Figure 1 in ref 23 as 47 ± 2 and 35 ± 2 cm^{-1}, respectively. However, the width of the stronger 578 nm band measured directly from the Figure 2 in the same ref 23 is larger (62 ± 5 cm^{-1}).

The PIC monomer band is much broader having the double value of the half-width at half-maximum (2hwhm) for the long-

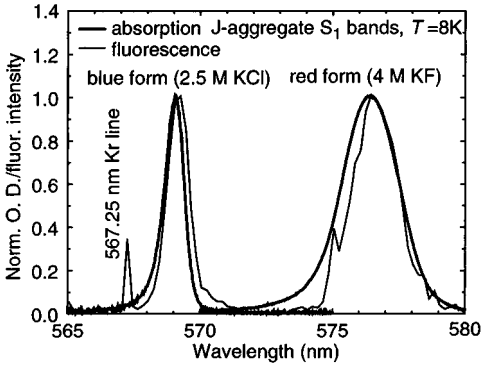

Figure 10. Absorption and fluorescence spectra of PIC (10^{-3} M) J-aggregates in 50% glycerol in the presence of 2.5 M KCl (blue form) and 4 M KF (red form), $T = 8$ K. The solution was placed in a 10 μm silica cell or between silica plates (3 μm layer) for absorption and fluorescence measurements, respectively. Slits (absorption/excitation/emission): 0.2/1.5/0.05 nm (blue form) and 0.5/1.5/0.1 nm (red form). The Stokes' sifts are 4 ± 1 cm^{-1} (blue form) and 6 ± 2 cm^{-1} (red form). The Kr emission lines (one appears at 567.25 nm) served for wavelength calibration.

wavelength side of the band of 764 and 1071 cm^{-1} in glycerol/water and PMMA at 8 K, respectively (Figures 3 and 11, Tables 1 and 3).

The inhomogeneous site-distribution functions (IDF) for monomeric and J-bands are of interest, since, at least in principle, the effective size of aggregates (exciton coherence length, delocalization volume) could be deduced on the basis of their ratio.[14] The fwhm of the absorption or fluorescence contour does not exceed the width of IDF more than by 10%, if the spectral band is composed mainly of zero-phonon lines (DWF > 0.5)[47] (see also ref 48). Because the Stokes' shift between the absorption and fluorescence band maxima is only about 10% of the bandwidth (Figure 10), the IDF of J-bands should nearly coincide with the bandwidth.

On the other hand, the weak 0−0 line of the PIC monomer in aza-PIC matrix is accompanied by a huge low-frequency wing having fwhm 300 ± 30 cm^{-1} (Figure 1 in ref 41). By subtracting this wing width from the measured bandwidth (764 cm^{-1}) one obtains that the IDF of PIC in glycerol/water host matrix cannot be much larger than ~400 cm^{-1}. Rigid molecules with similar size and dispersive solvent shifts, anthracene and moderately polar 9-cyanoanthracene in a polar propylene carbonate glass possess similar IDF widths of 300 and 560 cm^{-1}, respectively.[48] Consequently, the PIC monomer in vitreous solvents does not reveal excessive inhomogeneous broadening, despite the nonplanarity and flexibility of the chromophore. In polymers the absorption spectra are remarkably broader (Table 1 and Figure 1) because the interaction with macromolecules may result in additional inhomogeneous broadening owing to the geometry distorsions of PIC molecules.

Therefore, a narrowing of inhomogeneous bandwidth approximately by an order of magnitude takes place in J-aggregates. An attempt to derive the aggregate size from this factor would be justified if all the aggregated PIC molecules were exposed to matrix inhomogeneities (e.g., in a thin thread-like linear polymer). However, the thermal broadening and shift of the J-bands is insensitive with respect to the melting of the 50% glycerol matrix (subsections 5−7). Thus, it is highly probable, that the aggregate has a much more compact structure. Evidently, the hydrophobic interaction serves as a principle driving force of aggregation in aqueous environment and tries to minimize the water−pigment contact. One can treat the aggregate as an ordered particle, a kind of microscopic crystal. It is obvious that the role of motional narrowing (exciton

TABLE 3: Fitting Parameters for the Temperature Dependence of S_1 Bandwidth (Full Width at Half-Maximum) (Γ) of PIC Monomer and J-Aggregates

species	matrix	Γ(10 K) (cm^{-1})[a]	Γ(293 K) (cm^{-1})[a]	ΔΓ (cm^{-1})[b]	$\Gamma = a_0 + a_1 T^{a_2}$			ΔT (K)[c]
					a_0 (cm^{-1})	a_1	a_2	
monomer[d]	PMMA	1071 ± 5	1330 ± 10	259	1068	0.0051	1.91	9−324
					1067	0.0052	1.91	9−190
J-aggregate (blue form)	glycerol/H_2O (50%) + 2 M KCl	30 ± 0.2	140 ± 1	110	31	6.4×10^{-7}	3.34	13−294
					32	4.6×10^{-7}	3.32	13−190
J-aggregate (red form)	glycerol/H_2O (50%) + 4 M KF	78 ± 0.5	182 ± 1[e]	104	78	3.9×10^{-7}	3.42	8−273
					79	7.5×10^{-7}	3.26	8−190

[a] Bandwidth at 10 and 293 K, respectively. [b] Band broadening between 10 and 293 K. [c] Temperature interval of the fitting. [d] Double half-width at half-maximum (2hwhm) of the long-wavelength side of the band. [e] Extrapolated value.

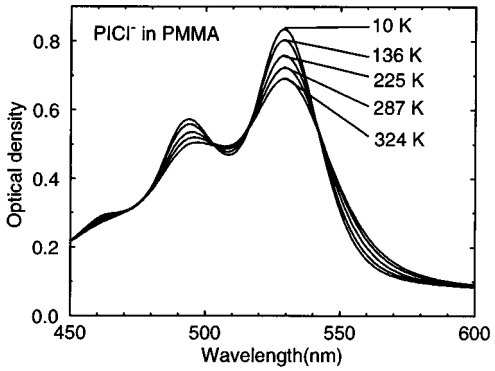

Figure 11. Temperature dependence of the 1,1′-diethyl-2,2′-cyanine iodide absorption spectrum in poly(methyl methacrylate) film.

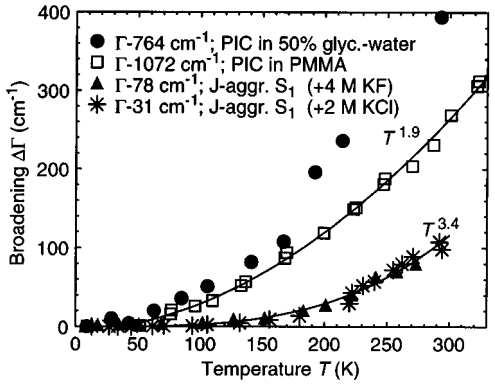

Figure 12. Temperature-induced broadening of PIC iodide absorption maxima in different systems (relative to 0 K): monomeric dye in 50% glycerol/water glass (●) and PMMA (□); the S_1 bands of the red (▲) and blue (∗) forms of the aggregates in 50% glycerol/water glass. Experimental data were approximated with power-law dependencies (parameters of the fitting curves are given in Table 3).

delocalization)[14,49] in determining the inhomogeneous bandwidth critically depends on the structure of the aggregate. Ordered structures such as microscopic crystals can have narrow exciton bands. Without detailed knowledge of the structure it is hardly possible to derive the size of aggregates (coherence volume of the exciton) from the ratio of bandwidths. Indeed, it was established in a recent study[50] that the narrowness of J-bands arises from the reduction of disorder upon aggregation, rather than a motional narrowing effect.

5. Thermal Band Broadening in PIC Monomer and J-Aggregates. The influence of temperature (*T*) on absorption bandwidth was studied in the broad *T* range between 10 and 300 K for PIC monomers in 50% glycerol/water and PMMA (Figure 11) as well as for J-aggregates (Figure 4). The experimental data can be approximated very well with power-law dependencies in the full *T* range from 10 to 270−330 K (Figure 12 and Table 3), except for PIC monomer in the glycerol/water mixture that shows a discontinuity at 180 K. A fast blue shift sets in at that *T* indicating the melting of the

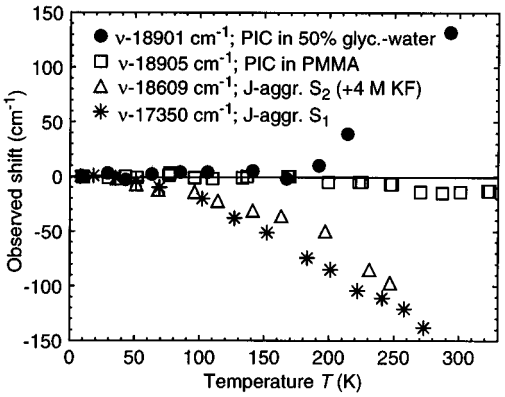

Figure 13. Temperature-induced shifts of 1,1′-diethyl-2,2′-cyanine iodide absorption maxima in different systems relative to 0 K: monomeric dye in 50% glycerol/water glass (●) and PMMA (□) and the S_1 (∗) and the S_2 (535 nm) bands (△) of J-aggregates in 50% glycerol/water glass in the presence of 4 M KF (red form).

sample (Figure 13). Broadening of the PIC monomer band in PMMA has a quadratic *T* dependence, whereas the J-band obeys a much steeper relationship with *T* coefficient 3.4. A similar correlation between the *T* coefficient of the band broadening and the linear electron−phonon coupling strength (DWF) can be followed for different π-electronic molecules embedded in polymer matrices (see below). In case of spectral bands consisting mainly of purely electronic zero-phonon lines (DWF > 0.7) (octaethylporphine and pyrene in poly(vinyl butyral) matrix) the *T* coefficient is as large as 2.5−3 ($80 < T < 300$ K) (data not shown). By contrast, for a predominately vibronic transition in β-carotene the *T* dependence of the band width has a shallow slope with *T* coefficient of 1.3−1.5.[29]

The steep *T*-dependencies above 140 K for both the blue and red forms of J-aggregates can also be approximated to an Arrhenius relationship with an effective activation energy of 520 ± 20 cm^{-1}. Vibrational lines with similar frequencies appear in the selective fluorescence spectra at 489 and 609 cm^{-1} (Figure 9). Therefore, the thermal population of local vibrational modes may contribute to the band broadening in PIC aggregates.

In our glycerol/water/salt system the thermal J-band broadening is about two times smaller than that of the red excitonic origin (at 576.1 nm) for PIC bromide aggregate in ethylene glycol/water glass (Table 4).[20] Moreover, the hole width between 30 and 80 K[22,23] exceeds the band broadening by a factor of 5 or more (Table 4). The width of persistent holes corresponds largely to the homogeneous line width determined by dynamic dephasing processes. The contribution of irreversible broadening of the holes during the burning/readout time as a result of spectral diffusion should be negligible, since the residual hole broadening after the temperature cycling is very small (0.3 cm^{-1} for the excursion temperature up to 80 K).[22,23] Note, that in an ideal case the increase of the bandwidth amounts to a half of the homogeneous hole width.

TABLE 4: Temperature Dependence of the Band/Hole Broadening ($\Delta\Gamma$) and the Observed Band Shift ($\Delta\nu_m$) in J-Aggregates[a]

	broadening $\Delta\Gamma$ (cm^{-1})				shift $\Delta\nu_m$ (cm^{-1})	
T (K)	blue form 568.9 nm (2 M KCl)	red form 576.4 nm (4 M KF)	576.1 nm band (ref 20)[b]	hole in 578 nm band (refs 22,23)[c]	both forms (568.9, 576.4 nm)	576.1 nm band (ref 20)[b]
30	<0.2	0.2	0.7	0.8	−2	−0.7
40	0.2	0.3	0.8	1.1	−3.5	−1.9
50	0.3	0.5	1.2	1.6	−5.5	−4.2
60	0.5	1	1.5	3.3	−8	−7
70	0.8	1.4	1.9	5.7	−11	−10.4
80	1.2	1.8	2.5	10; 0.3[d]	−15	−14
100	2	3.5	4.2		−22	−22
120	4	5	7.3		−33	−30
140	6.4	7.5	12		−44	−39
160	10	12	22		−58	−48
180	14	17	38		−73	

[a] Relative to that at 10 K, in 50% (w/w) glycerol/water with added salts. [b] PIC bromide in ethylene glycol/water glass; data are taken from Figure 2 in ref 20. [c] Quasihomogeneous hole width for PIC iodide J-aggregate in 50% (v/v) ethylene glycol/water glass; data are taken from Figure 5 in ref 22. [d] Broadening of a hole (burned and measured at 4 K) as a result of thermal cycling up to 80 K (from Figure 3 in refs 22 and 23).

In contrast to glycerol/water/salt system where aggregation takes place already at ambient conditions, the J-aggregates are formed in glycol/water mixture only upon cooling[25] or under the external pressure.[43] It is conceivable that the aggregates in glycol/water have a smaller size and, therefore, a larger area of surface at contact with polar glassy host matrix. In its turn, this may enhance the strength of electron-phonon coupling and lead to extensive broadening.

Despite larger inhomogeneous width the T broadening in the red form is only very slightly stronger than that in the blue form (Table 4). In summary, aggregates prepared upon addition of high concentration of electrolytes possess considerably smaller thermal broadening than those formed in the systems without salt.[20,22,23] The aggregates described above have probably the smallest homogeneous broadening between 8 and 80 K (~1 cm^{-1}) among the optical spectra of all the other molecular systems (i.e., neat molecular crystals, Shpolskii matrices, dyes in polymers, etc.).

6. Temperature Shift of PIC Monomer Band in PMMA. The $S_1 \leftarrow S_0$ transition of PIC in PMMA film undergoes a negligible bathochromic shift of 0.5 nm upon the warming up from 10 to 300 K (Figures 11 and 13). In water/glycerol mixture a fast hypsochromic shift sets in above the glass transition point around 200 K (Figure 13). Above 200 K, the density of the liquid decreases rapidly and the corresponding diminishing of matrix polarizability leads to a fast decrease of the dispersive shift. In PMMA the dispersive blue shift (upon the rise of temperature) and the phonon-induced or pure thermal red shift nearly compensate each other. The shift components can be separated, provided the thermal expansion coefficient of the matrix is known.[29]

We first calculate the temperature dependence of dispersive effect from the density and refractive index changes of PMMA (eq 2). The density relative to that at 0 K (d_T/d_0) was found by integrating the tabulated values of linear thermal expansion coefficients (a) for PMMA:[51]

$$d_T/d_0 = (1 + \int a\, dT)^{-3} \qquad (5)$$

With the refractive index value of PMMA at 293 K $n = n^{20}_D = 1.490$[35] ($\phi(n^2) = 0.289$) we obtain from eqs 2 and 5 that the Lorentz−Lorenz function $\phi(n^2)$ at 0 K is equal to 0.300. According to eqs 1, 2, and 5, the temperature dependence of the dispersive shift relative to that at $T = 0$ K can be calculated as

$$\Delta\nu_{disp} = -0.300p[1 - (1 + \int a\, dT)^{-3}] \qquad (6)$$

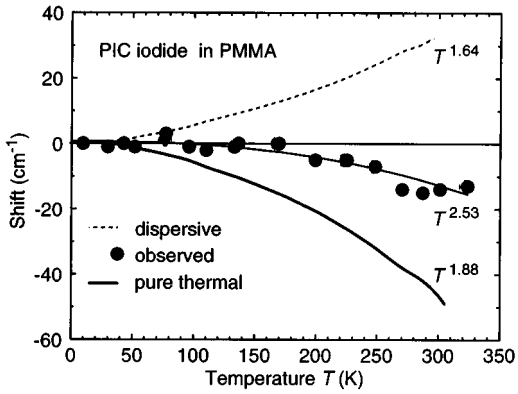

Figure 14. Dispersive (dotted line) and pure thermal (thick line) contributions to the observed temperature shift of PIC absorption maximum in PMMA relative to 0 K. Dispersive shift was calculated from eq 6 and subtracted from the observed shift (●) to obtain the pure thermal shift. The temperature coefficients of the power-law approximation are indicated (see Table 2).

Dispersive solvent effect always produces a blue shift upon rising the temperature as a result of volume dilatation of the matrix. The difference between the observed band shift and the calculated dispersive contribution yields the purely thermal (vibronic) part of the band shift (Figure 14, full line). The experimental shift and the calculated contributions can be very well fitted to power-law dependencies (Figure 14, Table 2).

7. Temperature Shift of J-Aggregate Bands. The aggregate bands shift strongly to longer wavelengths upon the increase of temperature (Figures 4 and 13, Table 2), in contrast to the PIC monomer absorption in PMMA that shows a very small net shift (Figures 11, 13, and 14).

The decomposition of thermal band shift into constituents is carried out as follows. First, the dispersive shift is calculated by assuming that both exciton levels possess a similar matrix polarizability dependence. Further, it is supposed that the solvent shift scales linearly with the density of the crystal.[52] Similarly, the shifts of excitonic components are determined from the excitonic splitting value at low temperature. The resonance interaction decreases as a result of thermal expansion, and the levels approach each other in a symmetrical fashion. Finally, the pure thermal effect on both exciton bands is estimated by taking into account the dispersive shift and the change of excitonic splitting of levels.

Recently the temperature changes of the unit cell parameters for bis(dimethylamino)heptamethinium perchlorate ($BDH^+ClO_4^-$) crystals have been measured by X-ray crystallography.[30] The

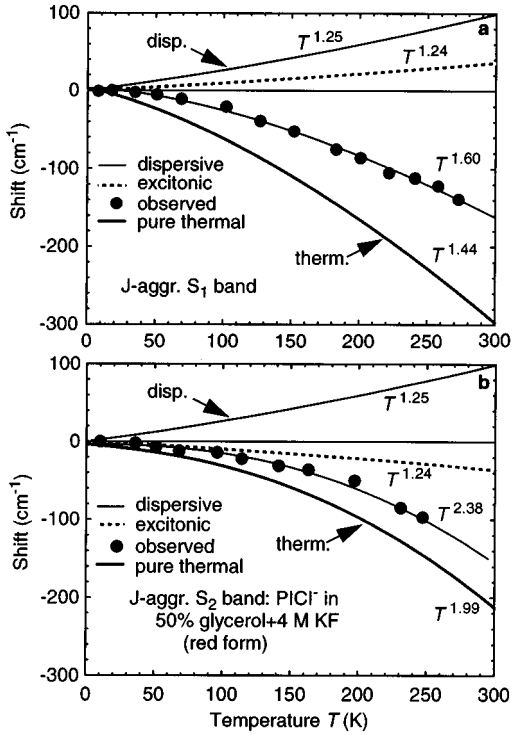

Figure 15. Temperature-induced shifts of the excitonic absorption bands for the red form of PIC aggregates in 50% glycerol/water glass in the presence of 4 M KF: (a) S_1 (576.4 nm) band, (b) S_2 (537.4 nm) band. The dispersive and excitonic shifts resulting from thermal expansion were calculated from eqs 8 and 9, respectively, and subtracted from the observed shift (●) to obtain the pure thermal contribution. The temperature coefficients of the power-law approximation are indicated (see Table 2).

thermal volume change has been described by the following polynomial regression:[30]

$$\Delta V/V_0 = 1.3 \times 10^{-4}\, T + 2.38 \times 10^{-7}\, T^2 \qquad (7)$$

Here we suppose that the PIC aggregates have the same relatively large thermal expansivity as $BDH^+ClO_4^-$ crystals (6% volume increase between 30 and 293 K).

The density-dependent dispersive ($\Delta\nu_{disp}$) component is calculated from the absolute shift of the S_1 and S_2 midpoint energy at $T = 0$ K (17 980 cm^{-1} for the red form) relative to the 0−0 frequency of nonsolvated PIC ν_0^0 (eq 1) (−1736 cm^{-1}) and the relative thermal expansivity ($\Delta V/V_o$) of the matrix (eq 7):

$$\Delta\nu_{disp} = 1736(\Delta V/V_0)/(1 + \Delta V/V_0) \qquad (8)$$

Similarly, the excitonic shift is taken equal for both exciton bands, but with a different sign:

$$\Delta\nu_{ex} = \pm{}^1/_2(1270)(\Delta V/V_0)/(1 + \Delta V/V_0) \qquad (9)$$

where 1270 cm^{-1} stands for exciton splitting. Sign + means that, with increasing temperature, the J-band is blue shifted. The opposite is true for the S_2 band of the upper exciton level. According to eq 9, the exciton splitting decreases by 70 cm^{-1} between 0 and 293 K.

Different shift components of the S_1 and S_2 bands for the red form of PIC aggregates are illustrated in Figure 15. The observed band shift and its constituents were approximated to a power-law dependence. The fitting parameters are given in Table 2. Between 8 and 190 K, the observed shifts of S_1 and S_2 bands obey very well a nearly quadratic dependence. The fits in the full T range are slightly worse and have the power coefficient for the S_1 band about 1.5. Pure thermal shifts which are of main interest from the point of view of EPC are characterized by $T^{1.5}$ to T^2 dependencies for the PIC monomer and both excitonic transitions. According to eqs 8 and 9 the $T^{1.25}$ dependence of dispersive and excitonic components reflects the thermal expansion of the crystal which turns out to be rather shallow (eq 7).[30]

TABLE 5: Temperature-Induced Pure Thermal Shift ($\Delta\nu_m^t$) and Broadening ($\Delta\Gamma$) of 0−0 Absorption Bands[a]

compound	$\Delta\nu_m^t$ (cm^{-1})	$\Delta\Gamma$ (cm^{-1})	$-\Delta\nu_m^t/\Delta\Gamma$	DWF[b]	$-p$ (cm^{-1})[c]
PIC J-aggregate	−220	104	2.1		
octaethylporphine	−90	60	1.5	0.87[d]	130 ± 20
pyrene	−65	80	0.8	0.75[e]	1160 ± 40
pheophytin *a*[f]	−60	70	0.86		980 ± 30[f]
HITCI[g]	−50	120	0.42	0.15[h]	3300 ± 400
tetracene	−40	110	0.36	∼0.4[h]	5100 ± 300
PIC iodide[i]	−30	240	0.13	0.01[j]	3000 ± 200
pheophytin *a* (Soret band)[f]	−15	180	0.08		4300 ± 300[f]
β-carotene[f]	60 ± 20	200	−0.3		9000 ± 700[f]

[a] Between 80 and 293 K in PVB matrix, error ±15%. [b] Debye-Waller factor. [c] Dispersive solvent shift per unity Lorentz−Lorenz function (slope of eq 1) from refs 27 and 28. [d] Reference 47. [e] Reference 48. [f] Reference 29. [g] 1,1′,3,3,3′,3′-hexamethylindotricarbocyanine iodide. [h] Reference 55. [i] In PMMA. [j] References 24 and 41.

The absolute values of pure thermal shifts of aggregate bands between 0 and 293 K are also much larger than these of the monomer (−200 to 300 vs −44 cm^{-1}). Bathochromic phonon-induced shifts are characteristic for zero-phonon lines in both organic[53] and inorganic[54] materials as well as for broad bands in doped polymers.[29] For comparison, the broadening and shift data between 80 and 293 K are presented in Table 5 for S_1 absorption bands of various π-electronic chromophores doped in poly(vinyl butyral) (PVB) film. The pure thermal shift was estimated as described above for PIC/PMMA. It follows from Table 5 that the shift is strongly correlated with the strength of linear EPC (DWF). For example, at first sight, surprising decrease of pure thermal shifts with increasing the EPC occurs for the S_1 bands in octaethylporphine (−90 cm^{-1}, weak EPC) > pyrene > pheophytin *a* > cyanine dye HITCI > tetracene > pheophytin *a* (Soret band) (−15 cm^{-1}, strong EPC). However, thermal shift of spectral holes burned in tetra-*tert*-butyl-tetraazaporhine embedded in various polymer hosts reveals a normal behaviour in the low-temperature range (7−50 K), (i.e., larger shifts were observed for systems with stronger EPC).[52]

To explain this discrepancy between the behavior of zero-phonon lines and broad bands, it can be proposed that at higher temperatures another shift mechanism sets in that compensates the initial red shift of zero-phonon lines, particularly in the systems with strong EPC. Indeed, in case of β-carotene in polystyrene or PVB matrix, the initial red shift is changed to a blue one above 110−160 K.[29] This effect can be accounted for in terms quadratic EPC, if the relevant "phonon" modes have higher frequencies in the excited state. When the excited-state polarizability (solvent shift) is large, the strengthening of intermolecular interactions in the excited state may result in the increase of the frequencies of quasilocal (intermolecular) vibrations in the excited state.[29] Furthermore, the intramolecular torsional modes in β-carotene and PIC monomer may have higher frequencies in the excited state. Most of the dye/polymer systems occupy an intermediate position between PIC monomer and aggregates, as far as the pure thermal shift and the strength of EPC are concerned (Table 5).

8. General Discussion of Electron−Phonon Coupling in Monomers and J-Aggregates. EPC manifests itself in the shift

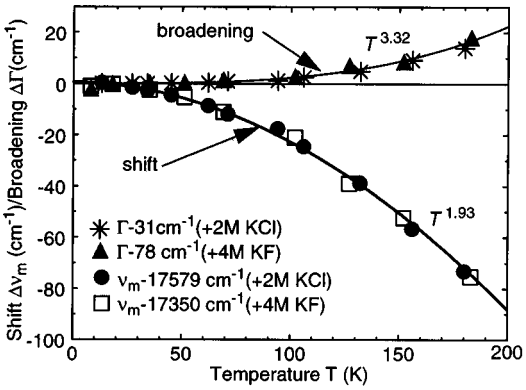

Figure 16. Comparison of the observed temperature shift (●, □) and broadening (∗, ▲) of J-bands in the blue (●, ∗) and red (□, ▲) forms of PIC aggregates in 50% glycerol/water glass in the low *T* region. Temperature coefficients of the power-law approximation between 10 and 190 K are indicated (see Tables 2 and 3).

and broadening of electronic transitions. The observed *T*-induced shift and broadening of sharp PIC aggregate bands are plotted in an enlarged scale in Figure 16. Note that the shift below 20 K and the broadening below 50 K are too small to be reliably determined in our spectrophotometric measurement. The behavior of the blue and the red forms is similar (Tables 2−4). As compared to the aggregate, the PIC monomer embedded in a PMMA film has a much smaller pure thermal shift (Figure 14) and a much stronger broadening (Figure 12) in the whole explored *T* interval.

Table 5 summarizes the broadening and shift data for different π-electronic chromophores in PVB host matrix. The magnitude of pure thermal shift ($\Delta\nu_m^t$) of J-aggregate bands is much larger than the broadening ($\Delta\Gamma$) between 80 and 293 K ($-\Delta\nu_m^t/\Delta\Gamma = 2.1$). The shift-to-broadening ratio is also larger than unity for octaethylporphine and decreases fast in the series of pheophytin *a* > pyrene > HITCI > tetracene > PIC monomer. It is evident that $-\Delta\nu_m^t/\Delta\Gamma$ is strongly correlated with the strength of linear EPC (DWF) and the dispersive solvent shift parameter *p* (the slope of eq 1). The DWF's were estimated earlier from the site selection spectra and hole-burning data.[55] The EPC characteristics of the PIC in monomeric and aggregated state constitute nearly the extreme cases among the organic systems from β-carotene to octaethylporphine.

According to the theory of impurity centers in crystals, the shift of a zero-phonon transition is linear with the quadratic EPC constant β, whereas the broadening is proportional to β^2.[56] Therefore, in case of weak EPC $\beta < 1$ and $\beta > \beta^2$ (i.e., the shift is larger than the broadening). The constant β determines the change of the normal phonon coordinates upon phototransition in the impurity or, in other words, the change of curvature of the harmonic potential between the ground and the excited state.[56]

Considering the EPC over a very broad *T* interval, three main groups of vibrational excitations can be discerned: delocalized phonon-like modes, intermolecular (quasilocal) vibrations, and the torsional or librational movements of the flexible chromophores themselves. The interaction with the first two types of vibrations can be sensitive to the changes of intermolecular van der Waals forces upon excitation, which in turn depend on the polarizability difference and electrical charge redistribution between the ground and the excited states. The same factors determine the magnitude of solvent shift. The interdependence of solvent shifts and EPC was first emphasized in ref 55 and further discussed in ref 29.

The most noticeable feature at the J-aggregation phenomenon is that a monomeric species that is strongly coupled to both intra- and intermolecular vibrations can give rise to a spectroscopic entity which is very weakly interacting with phonons and local modes. Obviously, only a very strong resonant interaction is able to decouple the exciton from the matrix modes and even local vibrations. Thus the first condition of primary importance seems to be the large oscillator strength of the transition (at least 0.5). In accordance with large oscillator strength of the Soret band, such a narrowing has been indeed observed in the aggregated porphyrins in acidic media.[57] Nevertheless, for similarly intense 1^1B_u-1^1A_g transitions in polyenes, in ^1B_b (β) bands in polycyclic hydrocarbons,[58] and 200−240 nm bands in fullerenes,[59] the J-aggregation effect has not been observed. The above mentioned transitions are characterized by huge dispersive solvent shifts ($-p$ > 8000 cm^{-1}/unity Lorentz−Lorenz function[28,29,59]) and, consequently, very large increase in polarizability of the excited state. On the other hand, the solvent shift in polymethines and the Soret bands in porphyrins is at least by a factor of 2 smaller ($-p$ = 3000−4000 cm^{-1}).[28,38,60] Bearing in mind the interrelationship between the EPC and the solvent shift, it appears that both the relatively small change of polarizability and the large transition dipole moment are necessary preconditions for essential decoupling of vibrational motions from the exciton which leads to the formation of a characteristic narrow-band spectrum of aggregated polymethine dyes and porphyrins. The influence of another crucial factor, the chemical structure, has been investigated already in the very first papers on aggregation properties of numerous monomethine and carbocyanine dyes[4,7] (see also ref 13).

Conclusions

Absorption and fluorescence properties of J-aggregates in the solution of 10^{-3} M PIC iodide in 50% (w/w) glycerol/water have been studied in the temperature interval from 8 to 293 K. Both the red and blue aggregate forms were prepared selectively in the presence of high concentration (2−4 M) of potassium fluoride and chloride or bromide. As a result, clean spectra of individual aggregate forms were be obtained. The broader features peaking at 535 and 495 nm were assigned to the transition involving the upper excitonic level (S_2) and its vibronic replica (S_{21}), respectively. The distance between the two transitions (exciton splitting) equals 1270 ± 10 cm^{-1} in both blue and red forms.

The thermal shift and broadening of exciton bands in PIC aggregates was investigated in a broad temperature range up to 293 K and compared to those for PIC monomer and other π-electronic molecules. The pure phonon-induced part of the shift was separated by subtracting the dispersive and excitonic contributions from the observed temperature shift. As far as the strength of electron−phonon coupling of optical transitions is concerned, the PIC monomers in polymer matrices (strong EPC) and in J-aggregates (very weak EPC) constitute essentially limiting cases of the van der Waals systems. Other π-electronic molecules (porphyrins, polymethine dyes, and aromatic hydrocarbons) in polymer environment possess intermediate strength of EPC.

For a dramatic reduction of the coupling strength to both the matrix and quasilocal vibrations occurring upon J-aggregation the relatively small polarizability change between the ground and the excited state seems to be crucial. Large change in $\Delta\alpha$ would inevitably produce a shift in intermolecular distances in the equilibrium state and the change of intermolecular force constants upon optical excitation. Accordingly, the S_1 bands in polymethine dyes and the Soret bands of porphyrins[57] that have relatively small solvent shifts can give rise to the spectral

narrowing upon aggregation, whereas strong transitions in polyenes, aromatic hydrocarbons and fullerenes probably cannot.

Finally, a complete scheme is proposed to illustrate how the 0−0 energy level of the cold nonsolvated PIC cation in vacuum is shifted and split in J-aggregates as a result of dispersive, excitonic, and vibronic interactions.

References and Notes

(1) Jelly, E. E. *Nature* **1936**, *138*, 1009.
(2) Scheibe, G. *Angew. Chem.* **1937**, *50*, 51; **1937**, *50*, 212.
(3) Scheibe, G.; Mareis, A.; Ecker, H. *Naturwissenschaften* **1937**, *25*, 474.
(4) Scheibe, G. *Kolloid-Z.* **1938**, *82*, 1; Scheibe, G.; Müller, R.; Schiffmann, R. *Z. phys. Chem. B* **1941**, *49*, 324.
(5) Scheibe, G.; Kandler, L. *Naturwissenschaften* **1938**, *26*, 412; Scheibe, G. *Z. Elektrochemie* **1941**, *47*, 73.
(6) Scheibe, G.; Schöntag, A.; Katheder, F. *Naturwissenschaften* **1939**, *27*, 499.
(7) Ecker, H. *Kolloid-Z.* **1940**, *92*, 35.
(8) Scheibe, G. *Z. Elektrochemie* **1948**, *52*, 283.
(9) Scheibe, G. In *Optische Anregung organischer Systeme*; Foerst, W., Jung, W., Eds.; Verlag Chemie: Weinheim, 1966; pp 109−159.
(10) Daltrozzo, E.; Scheibe, G.; Gschwind, K.; Haimerl, F. *Photogr. Sci. Eng.* **1974**, *18*, 441.
(11) Davydov, A. S. *Theory of Molecular Excitons*; Plenum: New York, 1971.
(12) Kasha, M.; Rawls, H. R.; El-Bayoumi, M. A. *Pure Appl. Chem.* **1965**, *11*, 371.
(13) Czikkely, V.; Försterling, H. D.; Kuhn, H. *Chem. Phys. Lett.* **1970**, *6*, 11.
(14) Knapp, E. W. *Chem. Phys.* **1984**, *85*, 73.
(15) Scherer, P. O. J.; Fischer, S. F. *Chem. Phys.* **1984**, *86*, 269.
(16) Knapp, E. W.; Scherer, P. O. J.; Fischer, S. F. *Chem. Phys. Lett.* **1984**, *111*, 481.
(17) Mattoon, R. W. *J. Chem. Phys.* **1944**, *12*, 268.
(18) De Boer, S.; Vink, K. J.; Wiersma, D. A. *Chem. Phys. Lett.* **1987**, *137*, 99.
(19) De Boer, S.; Wiersma, D. A. *Chem. Phys. Lett.* **1990**, *165*, 45.
(20) Fidder, H.; Terpstra, J.; Wiersma, D. A. *J. Chem. Phys.* **1991**, *94*, 6895.
(21) Hirschmann, R.; Köhler, W.; Friedrich, J.; Daltrozzo, E. *Chem. Phys. Lett.* **1988**, *151*, 60.
(22) Hirschmann, R.; Friedrich, J. *J. Chem. Phys.* **1989**, *91*, 7988.
(23) Hirschmann, R.; Friedrich, J. *J. Opt. Soc. Am. B* **1992**, *9*, 811.
(24) Pschierer, H.; Friedrich, J. *Phys. Status Solidi B* **1995**, *189*, 43.
(25) Cooper, W. *Chem. Phys. Lett.* **1970**, *7*, 73.
(26) Cooper, W. *Photogr. Sci. Eng.* **1973**, *17*, 217.
(27) Renge, I. *J. Photochem. Photobiol. A* **1992**, *69*, 135.
(28) Renge, I. *Chem. Phys.* **1992**, *167*, 173.
(29) Renge, I.; van Grondelle, R.; Dekker, J. P. *J. Photochem. Photobiol. A* **1996**, *96*, 109.
(30) Daehne, L.; Endriss, A.; Ihringer, J. *Chem. Phys. Lett.* **1994**, *224*, 91.
(31) Renge, I. In *Proceedings of the 2nd International Conference on Excitonic Processes in Condensed Matter*; Schreiber, M., Ed.; Dresden University Press: Dresden, 1996; pp 27−30.
(32) *Aldrich Catalog Handbook of Fine Chemicals 1994*−1995; Aldrich Chemical Company, Inc.: Milwaukee, WI.
(33) *Landolt-Börnstein. Zahlenwerte und Funktionen*; New Series; Springer: Berlin, 1991; Vol. IV, Part 6.
(34) Lide, D. R., Ed. *CRC Handbook of Chemistry and Physics*, 77nd ed.; CRC Press: Boca Raton, 1996; p 8-56.
(35) Seferis, J. C. In *Polymer Handbook*, 3rd ed.; Brandrup, J., Immergut, E. H., Eds.; Wiley: New York, 1989; pp VI−451.
(36) Samara, G. A.; Riggleman, B. M.; Drickamer, H. G. *J. Chem. Phys.* **1962**, *37*, 1482.
(37) Bakshiev, N. G.; Girin, O. P.; Piterskaya, I. V. *Opt. Spektrosk.* **1968**, *24*, 901 [*Opt. Spectrosc.* **1968**, *24*, 483].
(38) West, W.; Geddes, A. L. *J. Phys. Chem.* **1964**, *68*, 837.
(39) Böttcher, C. J. F. *Theory of Electric Polarization*; Elsevier: Amsterdam, 1973; Vol. I.
(40) Bridgman, P. W. *Proc. Am. Acad. Arts Sci.* **1948**, *76*, 71.
(41) Marchetti, A. P.; Scozzafava, M. *Chem. Phys. Lett.* **1976**, *41*, 87.
(42) Sundarajan, K. S. *Z. Kristallogr.* **1936**, *93*, 238; *Landolt-Börnstein. Zahlenwerte und Funktionen*; 6 Aufl., Bd. II, Teil 8; Springer: Berlin, 1962; p 2−288.
(43) Lindrum, M.; Chan, I. Y. *J. Chem. Phys.* **1996**, *104*, 5359.
(44) Misawa, K.; Ono, H.; Minoshima, K.; Kobayashi, T. *Appl. Phys. Lett.* **1993**, *63*, 577; *J. Lumin.* **1994**, *60*−*61*, 812.
(45) Kobayashi, T. *Mol. Cryst. Liq. Cryst. Sci. Technol. Sect. A* **1996**, *283*, 17.
(46) Marchetti, A. B.; Salzberg, C. D.; Walker, E. I. P. *J. Chem. Phys.* **1976**, *64*, 4693.
(47) Renge, I. Unpublished data.
(48) Renge, I.; Wild, U. P. *J. Lumin.* **1996**, *66*−*67*, 305.
(49) Knoester, J. *J. Chem. Phys.* **1993**, *99*, 8466.
(50) Durrant, J. R.; Knoester, J.; Wiersma, D. A. *Chem. Phys. Lett.* **1994**, *222*, 450.
(51) Lyon, K. G.; Salinger, G. L.; Swenson, C. A. *Phys. Rev. B* **1979**, *19*, 4231.
(52) Renge, I. *J. Chem. Phys.* **1997**, *106*, 5835.
(53) Laisaar, A. I.; Mugra, A. K.-I.; Sapozhnikov, M. N. *Fiz. Tverd. Tela* **1974**, *16*, 1155 [*Sov. Phys. Solid State* **1974**, *16*, 741].
(54) Imbusch, G. F.; Yen, W. M.; Schawlow, A. L.; McCumber, D. E.; Sturge, M. D. *Phys. Rev. A* **1964**, *133*, 1030.
(55) Renge, I. *J. Opt. Soc. Am. B* **1992**, *9*, 719.
(56) Osad'ko, I. S.; Personov, R. I.; Shpol'skii, E. V. *J. Lumin.* **1973**, *6*, 369.
(57) Ohno, O.; Kaizu, Y.; Kobayashi, H. *J. Chem. Phys.* **1993**, *99*, 4128. Pasternack, R. F.; Schaefer, K. F.; Hambright, P. *Inorg. Chem.* **1994**, *33*, 2062. Akins, D. L.; Zhu, H.-R.; Guo, C. *J. Phys. Chem.* **1994**, *98*, 3612. Maiti, N. C.; Ravikanth, M.; Mazumdar, S.; Periasamy, N. *J. Phys. Chem.* **1995**, *99*, 17192.
(58) Klevens, H. B.; Platt, J. R. *J. Chem. Phys.* **1949**, *17*, 470.
(59) Renge, I. *J. Phys. Chem.* **1995**, *99*, 15955.
(60) Renge, I. *J. Phys. Chem.* **1993**, *97*, 6582.
(61) In ref 27, Table 3, the polarity correction was taken with the wrong sign. The correct values of ν_0^0 should read: rhodamine 6G, 19620 cm^{-1}; oxazine 4, 17380 cm^{-1}; resorufin, 17840 cm^{-1}, and HITCI, 13840 cm^{-1}.